Indian Journal of Pure & Applied Physics
Vol. 63, October 2025, pp. 882-891
DOI: 10.56042/ijpap.v63i10.11386

Estimating the Influence of Cumulus Parametrization Schemes in Simulation of Super Cyclonic Storm 'Amphan' Over The Bay of Bengal Using WRF-ARW Model

Arun Kumar[a,b,*], Sushil Kumar[b], Nagendra Kumar[a], Nitin Lohan[b] & Reena Nupur[c]

[a]Department of Mathematics, M M H College, Ghaziabad 201 001, India

[b]Department of Applied Mathematics, Gautam Buddha University, Greater Noida 201 312, India

[c]Symbiosis Centre for Management Studies, Noida Campus, Symbiosis International (Deemed University), Pune 412 115, India

Received: 26th May 2024 ; accepted: 25th August 2025

Tropical cyclone 'Amphan,' originating over the Bay of Bengal, made landfall as a well-defined low-pressure system across northern Bangladesh and the surrounding region around midnight on May 21, 2020. This research focuses on the influence of cumulus parameterization schemes (CPS) within the Advanced Research Weather Research Forecast (WRF-ARW) model for tropical cyclone 'Amphan.' Parameters such as maximum sustained wind (MSW), mean sea level pressure (MSLP), potential vorticity (PV), vertical integrated moisture transport (VIMT), and rainfall are investigated in this paper. This study employs the National Center for Environmental Prediction (NCEP)'s global operational analysis and prediction products at a 1°×1° resolution for initial and boundary conditions. The analyses compare different cumulus parameterization schemes Kain Fritsch (KF) Scheme, Betts-Miller-Janjic (BMJ), Grell-3, combined with the Yonsei University (YSU) planetary boundary layer (PBL) scheme and NCEP operational cloud microphysics scheme (Ferrier), against observed datasets from the Indian Meteorological Department (IMD) and ERA5 reanalysis datasets. Using the mass flux type scheme for cumulus parameterization, the results of MSW and MSLP with the Grell-3 scheme in WRF-ARW model are closely aligned with IMD observations during intense stages of tropical cyclone 'Amphan'. The findings highlight the efficacy of the Grell-3 cumulus parameterization scheme in capturing the large-scale Latitude versus height structure of PV. This research investigates the vertically integrated moisture transport (VIMT) for the SuCS 'Amphan' and its correlation with rainfall over BoB from 16-21, May 2020 using WRF-ARW simulated datasets and ERA5 reanalysis datasets. The Grell-3 scheme exhibits notable differences in the area-averaged VIMT and corresponding rainfall. This research contributes to enhancing the understanding and prediction accuracy of tropical cyclones through comprehensive WRF-ARW model analyses.

Keywords: Tropical cyclone, WRF-ARW model, SuCS amphan, Cumulus parameterization

1 Introduction

The North Indian Ocean includes both Bay of Bengal (BoB) and Arabian Sea (AS). The Bay of Bengal (BoB) and the Arabian Sea (AS) collectively contribute to approximately 7 % of tropical cyclones (TCs) over the world[1]. Both (BoB and AS) the basins are prominently prone for the occurring of Tropical Cyclones (TCs). However, the frequency of TCs is more in BoB as compared to AS[1]. TCs are responsible for heavy loss of life, and damaging the basic infrastructure over the large area of coastal states of India in the past 30 decades. The reasonably accurate prediction of track, intensity, and associated storm surges of these devasting storms are needed before at least 48 hours for planning and implementation the planning to save the life and property. The occurrence of tropical cyclones is attributed to factors such as bathymetry, dynamical characteristics over NIO, socio-economic conditions, and dense population. Notably, non-landfalling TCs are more prevalent than landfalling TCs over the BoB, with 8 out of 10 very severe TCs globally observed in the BoB and AS[1]. Understanding the complex dynamics of TCs is crucial for prediction and simulation. Numerical weather prediction (NWP) models have become an important tool in providing accurate data on tropical cyclones (TCs) strength and tracks.

Efforts are made to improve model performance, which involve strategies such as nested domains, refinement of initial and boundary conditions (IBCs), and adjustments to physical parameterizations.

*Corresponding author: E-mail: mr.arun.gautam@gmail.com

Among these, planetary boundary layer (PBL) and surface fluxes of heat, moisture, and momentum play a significant role. In some studies, it was emphasized that the importance of cumulus parameterization schemes (CPS) in modelling of tropical cyclones, as convection significantly influences their progression and intensification[2,3]. Several convective parameterization schemes, namely, the Kain–Fritsch new Eta scheme, Betts–Miller–Janjic scheme, and Grell-3 scheme are accessible within the WRF-ARW modelling system[4-8]. The Grell-3 scheme is obtained from the Grell–Devenyi ensemble scheme[8]. Grell Frietas scheme is based on scale aware mass flux scheme approach[9]. Kain Fristch (KF) scheme approach is based on mass flux with trigger and plume model[10]. Kain and Fritsch, studied the dependency of cumulus parameterization schemes on sub-grid precipitation rates, latent heat release, and the redistribution of thermodynamic and dynamic variables[10]. Weisman *et. al*., studied the effect of vertical wind share on the structure and evolution of convective storms[11]. Cumulus parameterization schemes can be disabled for grid resolutions less than 4 km, while microphysics schemes can resolve cloud and precipitatiom[11].

Initial implementations were focused on classic mass-flux and adjustment schemes such as Kain–Fritsch (KF), Betts–Miller–Janjic (BMJ), and Grell–Dévényi (GD)[12]. Raju *et al*., have conducted the sensitivity analyses to increase the prediction accuracy of tropical cyclone 'Nargis.'[13] Scale-aware and ensemble-based variants like Grell–Freitas (GF) and multi-scale KF were introduced to better accommodate simulations in the "gray zone" of convection at grid spacings between 5–10 km[9-14]. These developments were essential for regional and mesoscale modelling, where sensitivity to cumulus parameterization schemes (CPS) significantly impacts rainfall simulations and storm structure, especially in monsoon or cyclone-prone regions[15,16]. Further studies over diverse terrains including semi-arid regions of China, coastal Vietnam, the Indian subcontinent, and the Iberian Peninsula have evaluated newer schemes such as KF-CuP, GF, and modified Tiedtke options, revealing variable performance depending on regional dynamics and model resolution[17-19]

Singh *et al*., examined the dynamics and underlying factors associated to Super Cyclonic Storm (SuCS) Amphan, as well as its effects on aerosol redistribution along the four cities of the eastern coast and northeastern India[20]. Kumar *et al*., used the WRF-ARW model to study the features of super cyclonic storm "Amphan," and the results were compared against ERA5 reanalysis data[21]. The findings established the foundation for further sensitivity analysis and data assimilation studies by showing strong agreement in wind dispersion and moisture transport[21]. Kumar *et. al*, evaluated the performance of various microphysics schemes using the WRF model's 4D-VAR data assimilation system[22]. The Lin *et al*. scheme showed the most accurate course prediction and the best moisture transfer during the storm's most intense phase[22].

To analyse SuCS 'Amphan', three experiments are conducted in this paper using the WRF-ARW model with three different cumulus parameterization schemes and other fixed configurations. The primary objectives are to analyse maximum sustained wind (MSW), mean sea level pressure (MSLP), potential vorticity (PV), vertical integrated moisture transport (VIMT), and impact of VIMT on rainfall to understand the intensity and behaviour of SuCS 'Amphan.' The validation of results, namely, maximum sustained wind (MSW) and mean sea level pressure (MSLP) is made with IMD observational datasets and the validation of results, namely, potential vorticity (PV), vertically integrated moisture transport (VIMT), and rainfall is made with ERA5 reanalysis datasets. The paper is organized as follows: section 2 provides a description of SuCS 'Amphan.' section 3 outlines the experimental design, datasets, and methodology. A detailed discussion of the results, conclusions are provided in section 4 and 5, respectively.

2 Description of the Super Cyclonic Storm – 'Amphan'

Tropical cyclone 'Amphan' originated over the south Andaman sea, gradually advancing towards the southeast Bay of Bengal (BoB) on May 13, 2020. Initially classified as a deep depression (DD) over the southeast BoB by May 16, 2020, it swiftly intensified, reaching the status of a cyclonic storm (CS) to severe cyclonic storm (SCS) on the morning of May 17, 2020. The system evolved further, becoming a very severe cyclonic storm (VSCS) by the afternoon of May 17, 2020 an extremely severe cyclonic storm (ESCS) on the morning

of May 18, 2020 and ultimately achieving SuCS classification around the afternoon of May 18, 2020.

Maintaining its formidable strength, SuCS 'Amphan' lingered over the west-central BoB for nearly 24 hours. However, signs of weakening became apparent around the afternoon of May 19, as it transformed back into an ESCS over the same region. The storm proceeded to weaken further while traversing the west Bengal-Bangladesh coasts, reaching VSCS status near the Sunderbans between 1530-1730 UTC on May 20, 2020. During this critical period, the storm exhibited relentless winds with speeds ranging from 155-165 km/h, and gusting upto 185 km/h. The landfall of SuCS 'Amphan' occurred over the BoB very close to Kolkata on the night of May 20, 2020.

SuCS 'Amphan' gradually diminished into a SCS towards the northeast over Bangladesh on the midnight of May 20, 2020. Further degradation occurred, leading to its reclassification as a CS on the morning of May 21. By noon on May 21, 'Amphan' had weakened into a DD over Bangladesh, marking the conclusion of its impactful journey.

3 Data used and Methodology

3.1 Data used

The focused area of present study is Bay of Bengal (BoB) region, specifically within the geographical constraints of 78 °E to 103 °E longitude and 4 °N to 26 °N latitude. The 9 km horizontal grid resolution is kept for the selected region. The model simulation is conducted using a single domain covering a period of 126 hours for the aforementioned geographical region.

National Centre for Environmental Prediction (NCEP) operational analysis with a horizontal resolution of 1° × 1° is used for initial and boundary conditions to simulate the super cyclonic storm (SuCS) 'Amphan'. Lateral boundary conditions are acquired from NCEP Global Forecast System (GFS) forecast fields, downloaded at 6-hour intervals. For the purpose of validating the parameters, namely track, MSW, and MSLP obtained from the model integration, observational datasets from the India Meteorological Department (IMD) are utilized. These IMD datasets contribute to the assessment and verification of the accuracy and reliability of the model-generated results. The IMD observational datasets are used as a crucial layer of validation to the study. Validation is performed to assess the alignment of model outputs with observed meteorological conditions during the occurrence of SuCS 'Amphan.'

3.2 Methodology

The non-hydrostatic WRF-ARW model version 4.1.2 simulations outputs are used in this study. Runge-Kutta 2nd and Runge-Kutta 3rd order schemes are used to perform time integration, while advection is handled with 2nd to 6th order schemes. The model design with a focus on finer horizontal grid resolutions of a few kilometres or less is utilizing nested domains to predict and simulate various mesoscale atmospheric phenomena[23,24]. The detailed configuration of the model for simulating Super Cyclonic Storm (SuCS) Amphan is presented in Table 1.

The formula for Ertel's potential vorticity (PV), is given as follows:

$$q = \frac{1}{\rho}\eta.\nabla\theta\# \quad \ldots (1)$$

Table 1 — The detailed configuration of the model for simulating Super Cyclonic Storm (SuCS) Amphan.

Model Configuration	Configuration
	Bay of Bengal
Dynamics	Nonhydrostatic
Model domain	4 °N-26 °N, 78 °E-103 °E
Center of the domain	15 °N and 89.5 ° E
Horizontal grid distance	9 km
Map projection	Mercator
Horizontal grid system	Arakawa C-grid
Integration time step	40 s
Vertical coordinates	Terrain-following hydrostatic pressure vertical coordinate with 51 vertical levels
Time integration schemes	3rd order Runga-Kutta Scheme
Spatial differencing scheme	6th order center differencing
Micro physics	Ferrari
Radiation schemes (ra_lw_physics & ra_sw_physics)	Rapid radiative transfer model (RRTM) scheme for long wave/ Dudhiya for short wave
Surface layer parameterization (sf_surface_physics)	Thermal diffusion scheme
Planetry boundary layer physics (bl_pbl_physics)	YSU
Cumulus scheme (cu_physics)	Kain Fritsch (KF) Scheme (P1C11), Betts-Miller-Janjic (BMJ) (P1C22), Grell-3 (P1C55)

where ρ, η, θ, and represent the density, three-dimensional absolute vorticity vector, and potential temperature respectively[25].

Schubert and Alworth, performed numerical modelling of tropical cyclones and observed the vertical structure of tropical depressions contrasts with the deep PV columns in matured tropical cyclone[26]. Numerous observational studies have suggested that the potential vorticity (PV) within mature tropical cyclones (TCs) tends to maintain a uniform amplitude, extending from the surface to the upper troposphere[27,28].

Yau *et al*., observed a bottom-heavy PV structure and maximum values of PV in mature TCs. Bell and Montgomery (2008) studied a bottom-heavy PV structure using field campaign observations, and pointed out a bimodal structure with peaks at 1 and 3 km altitude[30]. Hausman *et al*., performed a numerical simulation of hurricane and demonstrated a bottom-heavy PV only when latent heating because of ice was deactivated, with a mid-tropospheric PV maximum appearing when this effect was considered[31]. Wang, and Rogers, found mid-tropospheric PV maxima in their numerical simulations of mature TCs, diverging from the bottom-heavy structure.

Stewart, explored the dynamics of ocean currents, elucidating their profound impact on global climate systems[34]. Through meticulous analysis of oceanic circulation patterns, the research uncovers crucial insights into the intricate interplay between the ocean and the Earth's climate. Trenberth *et al*. (2011) gave the formula for atmospheric conservation of moisture equation when vertically integrated in flux form as follows:

$$\frac{\partial w}{\partial t} + \nabla.\frac{1}{g}\int_0^{p_s} qVdp = E - P\# \quad \ldots (2)$$

where q is the specific humidity, V is the wind vector, w = $\frac{1}{g}\int_0^{p_s} qdp$ is the precipitable water (total column water vapor), p is pressure, p_s is the surface pressure, and g is the gravitational constant, E is the surface evaporation, and P is the net surface precipitation rate[35].

The moisture conservation equation in flux form of vertical integration suggested by Trenberth *et al*. is

$$\frac{\partial w}{\partial t} = -\nabla.\frac{1}{g}\int_0^{p_s} qVdp + E - P + R\# \quad \ldots (3)$$

where, R is the run off. The right-hand side of Eq. (3) is the difference between evaporation and precipitation, vertically integrated moisture flux divergence (VIMD) and runoff[36-38]. The tendency term is small for long-term means; this is recommended by Mo and Higgins (1996). So, Eq. (3) is now:

$$\nabla.\frac{1}{g}\int_0^{p_s} qVdp = E - P\# \quad \ldots (4)$$

Eq. (4) is the principal balance between E - P and vertically integrated moisture divergence[35].

The wind vector, V, is defined by $V = (u, v)$, where u and v are the east-west and north south components of wind. The vertical integrated moisture flux (Q) is calculated by the equation

$$Q = \frac{1}{g}\int_0^{p_s} qVdp\ \# \quad \ldots (5)$$

To determine the Vertical Integrated Moisture Transport (VIMT), vertical integration of this equation is performed from surface pressure (in hPa) to 300 hPa. This upper limit is chosen because specific humidity has a negligible effect above this level[39].

4 Results and Discussion

The following results are obtained using WRF model with 9 km resolution in a single domain over BoB. The following parameters viz maximum sustained wind (MSW), mean sea level pressure (MSLP), potential vorticity (PV), vertical integrated moisture transport (VIMT), and rainfall are analysed. MSW and MSLP are validated with IMD observational datasets, and PV, VIMT, and rainfall are compared with ERA5 reanalysis datasets. The detailed discussion is given in sections 4.1, 4.2, 4.3, and 4.4.

4.1 Simulation of Maximum Sustained Wind and Mean Sea Level Pressure

The SuCS 'Amphan' intensity is examined by considering mean sea level pressure (MSLP) and maximum sustained wind (MSW), using three different cumulus parameterization schemes (CPS) Kain Fritsch (KF) Scheme, Betts-Miller-Janjic (BMJ), Grell-3. The temporal progression of the observed and simulated by model (up to 126 hours) MSLP and MSW is depicted in Figs. 1-2. The observed lowest mean sea level pressure, recorded at 920 hPa on May

18, 2020, at 1800 UTC, for comparison. The minimum value of MSLP captured by Grell-3 scheme is 930 hPa on May 20, 2020, at 0000 UTC, while the minimum value captured by KF and BMJ schemes are 936 hPa and 935 hPa on May 20, 2020, at 0000 UTC and May 20, 2020, at 0600 UTC correspondingly. Thus, minimum value of MSLP captured by Grell-3 scheme is more closed to the observation than KF and BMJ scheme. It is evident that the Grell-3 scheme, closely predict the mean sea level pressure intensity, aligning well with the IMD observed values during intense stages (ESCS-VSCS-SuCS-VSCS-ESCS) of tropical cyclone 'Amphan'. However, the KF scheme exhibits better simulation around 24 hours before the cyclone's landfall. In comparison with Grell-3 scheme, the schemes KF, and BMJ, are unable to simulate well the MSLP intensity during the intense stages.

The maximum sustained wind, simulated by the WRF-ARW model using three different cumulus parameterization schemes (CPS) Kain Fritsch (KF) Scheme, Betts-Miller-Janjic (BMJ), Grell-3 at 0600 UTC on May 16, 2020, along with corresponding observations from IMD, is presented in Fig. 2. The highest value of maximum sustained wind (MSW) at SuCS stage, obtained from IMD, is approximately 67.01 m/s on May 18, 2020, at 1800 UTC. The KF scheme simulates a highest value of MSW of 55.45 m/s, on May 20, 2020, at 0000 UTC, while the BMJ, and Grell-3 schemes simulated highest value of MSW are 50.45 m/s, on May 20, 2020, at 0600UTC, and 53.22 m/s on May 19, 2020, at 1800UTC. In comparison with the IMD observed value, the KF, BMJ, and Grell-3, schemes underestimate the highest value of MSW during intense stages (VSCS-ESCS-SuCS-ESCS-VSCS). The KF scheme proves effective in representing sub-grid scale features related to updraft and downdraft processes, contributing to the development of strong convection. On the other hand, the BMJ convective adjustment scheme and the Grell-3 ensemble cumulus parameterization schemes exhibit deficiencies in low-level convergence, resulting in reduced convective activity during the cyclonic system's development. This underscores the significance of convective processes in predicting cyclone intensity. However, Grell-3 scheme shows highest value of MSW during intense stage (VSCS-ESCS-SuCS-ESCS-VSCS) of tropical cyclone 'Amphan'. The results indicate that the combination of the Grell-3 convection scheme exhibits superior predictive accuracy concerning both intensity and the approximate timing of landfall when compared to other schemes. Furthermore, an analysis of the cyclone's structure in terms of potential vorticity is conducted in Section 4.2 to comprehend the dynamical aspects.

The error analysis for SuCS Amphan's maximum sustained wind reveals distinctive performance variations among different convection schemes. The KF convection scheme and Grell-3 exhibit MSW root mean square error (RMSE) of approximately 11.31 m/s and 11.51 m/s, respectively. Though KF scheme is showing improved predictions, in terms of MSW RMSE, however, Grell-3 scheme is better for prediction because of its closeness to observed data during intense stages and overall RMSE is also very close to KF scheme. On the other hand, the BMJ scheme exhibits a less favourable, with high value of MSW RMSE (13.28 m/s).

The mean sea level pressure error analysis further highlights the performance disparities among

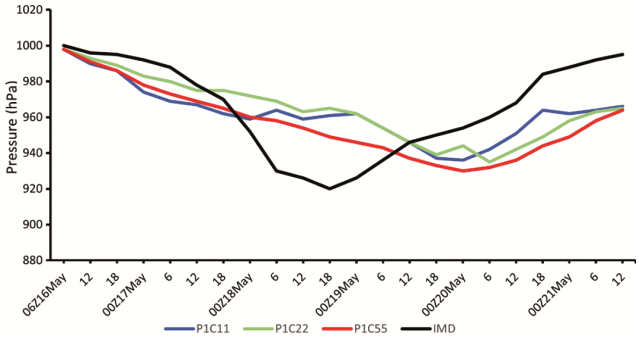

Fig. 1 — Time-evolution of tropical cyclone 'Amphan' intensity using WRF-ARW experiment data with combination of three Cumulus Parameterization Schemes KF (P1C11), BMJ (P1C22), and Grell-3 (P1C55) and IMD observed datasets for mean sea level pressure (hPa) from pre landfall (16 May 2020) to post landfall (21 May 2020)

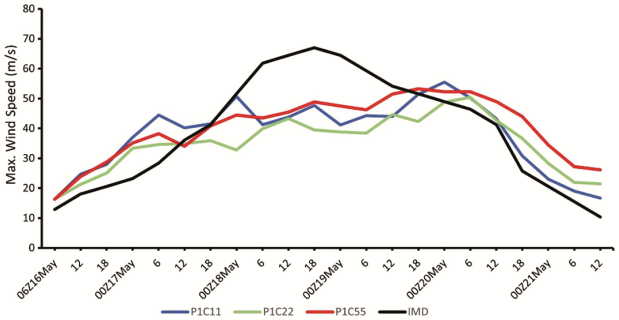

Fig. 2 — Time-evolution of tropical cyclone 'Amphan' intensity using WRF-ARW experiment data with combination of three Cumulus Parameterization Schemes KF (P1C11), BMJ (P1C22), and Grell-3 (P1C55) and IMD observed datasets for maximum sustained wind (m/s) from pre landfall (16 May 2020) to post landfall (21 May 2020)

convection schemes for SuCS Amphan. The KF convection scheme and Grell demonstrates bettere predictive capabilities with a mean sea level pressure error of 21.73 hPa and 22.91 hPa, respectively. The BMJ scheme exhibits a mean sea level pressure error of approximately 23.89 hPa. Though, these errors indicate notable deviations from the actual mean sea level pressure values, suggesting that both the BMJ and Grell3 schemes are less effective in predicting the MSLP of SuCS 'Amphan' compared to the KF scheme, however, Grell-3 scheme shows better predictive capability during intense stages.

4.2 Potential Vorticity Analysis

The analysis of Latitude versus height structure of potential vorticity (PV) at longitude 86.2 ^{o} from WRF-ARW model simulated data using three different cumulus parameterization schemes Kain Fritsch (KF) Scheme, Betts-Miller-Janjic (BMJ), Grell-3 and ERA5 reanalysis datasets on 18 May, 2020, 0600 UTC is shown in Fig. 3. The specified longitude and time are crucial for analysis as tropical cyclone 'Amphan' intensified into a Super Cyclonic Storm at that specific position and time. Figure 3 illustrates the shaded area, presenting the composite mean potential vorticity (PV) calculated on isobars through the utilization of three-dimensional absolute vorticity and θ gradient. Across all schemes of WRF-ARW model, the PV demonstrates a primary peak with an intensity of 8 PV units (PV units; 1 PVU = 10^{-6} K.m^{2}.kg^{-1}. s^{-1}) at approximately 450 hPa, accompanied by a secondary peak of 7.5 PVU in the lower troposphere, close to 850 hPa. The Grell-3 Fig. 3 (c) scheme provides strong rising motion extended up to 200 hPa height from latitude 12N to 13N, but underestimate the PV values captured by ERA5 reanalysis datasets Fig. 3 (d). On the other hand, from Fig. 3 (b-c), the KF convection scheme provide strong rising motion extended up to 300 hPa height from latitude 12.5 N to 14.5 N and around 15.5 N and the cumulus schemes employed by BMJ simulated vigorous upward motion extending up to a height of 350 hPa from latitude 12N to 13N and around 10.5 N, 11.5 N, 15 N. From Fig. 3 (a-d), in all the panels of Fig. 3, the high value of PV captured by BMJ scheme, covers more area horizontally than KF and Grell-3 schemes, while Grell-3 scheme captured high of PV goes up to more height than KF and BMJ

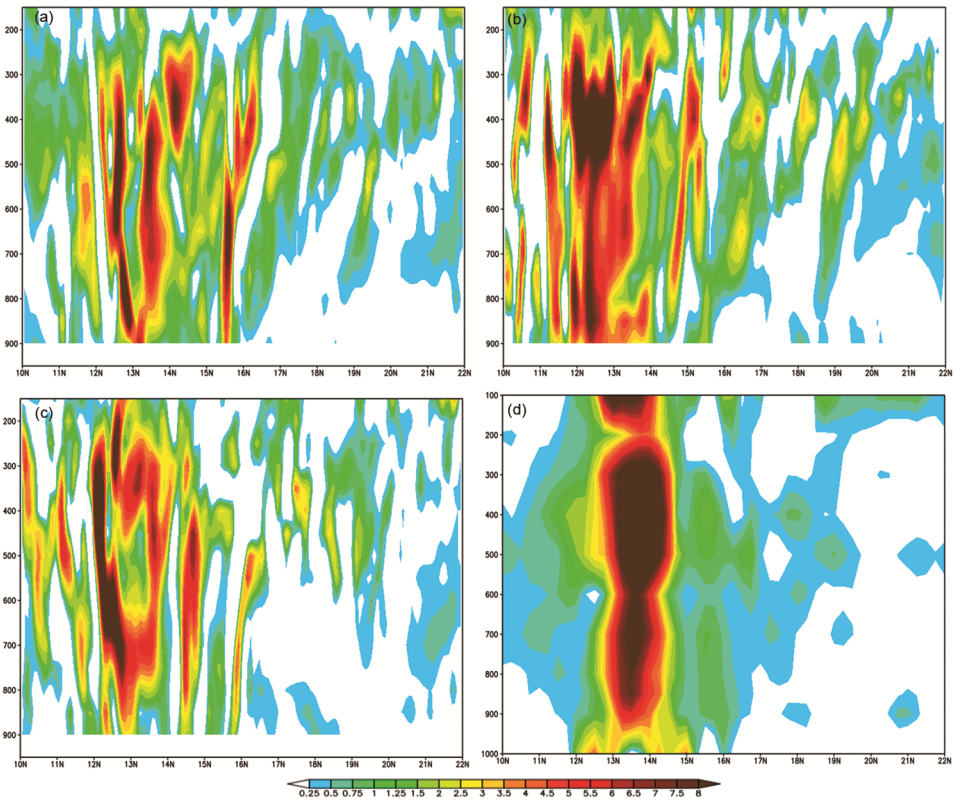

Fig. 3 — Latitude versus height structure of Potential Vorticity at 54 h of forecast on 18 May, 2020, 0600 UTC with three different cumulation parameterization schemes (a) KF (b) BMJ (c) Grell-3 using WRF-ARW experiment data and ERA5 reanalysis datasets (d) ERA5

schemes as compared to ERA5 reanalysis datasets. Thus, the BMJ scheme overestimates the PV value captured by ERA5 reanalysis datasets horizontally. The simulated outcomes suggest that all three CPS facilitate deep convection, marked by robust updrafts and downdrafts throughout the atmospheric column. However, PV values captured by Grell-3 scheme is more aligned to ERA5 reanalysis datasets.

4.3 Vertical Integrated Moisture Transport (VIMT) Analysis

The temporal variation of vertically integrated (surface to 300 hPa) moisture transport (VIMT) with three different cumulus parameterization schemes Kain Fritsch (KF) Scheme, Betts-Miller-Janjic (BMJ), Grell-3 and ERA5 reanalysis datasets, averaged over a domain of 85 °– 110 °E; 10 °– 20 °N, is shown in Fig. 4. All the three-parameterization schemes overestimated the VIMT value captured by ERA5 reanalysis datasets. The Grell-3 scheme shows a distinct pattern compared to BMJ and KF cumulus convection schemes, particularly during the mature stage. Grell-3 exhibits an increasing trend over the 6-hour simulation, reaching at highest value around the cyclone landfall (1523.6 kg m^{-1} s^{-1}). While, KF and BMJ exhibit an upward trend, the magnitude of VIMT is not as pronounced as that simulated by the Grell-3 scheme.

Simulations using BMJ and Grell-3 schemes indicate consistently low VIMT after 17 May 2020 at 1800 UTC. The KF parameterization scheme suggests a slight increase in VIMT from 16 May 2020 1200 UTC to 17 May 2020 1200 UTC. Consequently, considering the performance of these cumulus parameterization schemes, a comprehensive examination with various microphysics schemes and comparison with more reanalysis datasets is required for a better thorough understanding.

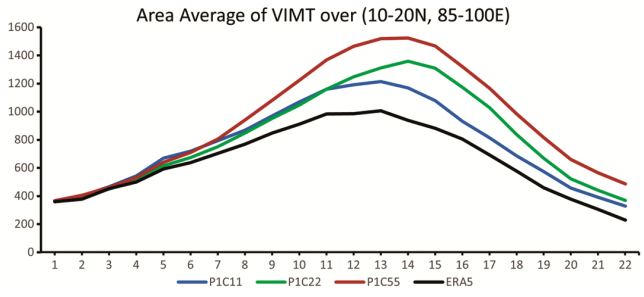

Fig. 4 — Area Average of vertically integrated moisture transport from pre landfall (16 May 2020) to post landfall (21 May 2020) using three different cumulus parameterization schemes KF (P1C11), BMJ (P1C22), and Grell-3 (P1C55) of WRF-ARW experiment data and ERA5 reanalysis datasets

4.4. Rainfall

The 24-hour accumulated rainfall valid at 0000 UTC on 17-20, May 2020, derived from ERA5 reanalysis (bottom panel) and from simulated 24-hour accumulated rainfall corresponding to the above period using WRF-ARW model with three different cumulus parameterization schemes (Kain Fritsch (KF) Scheme (P1C11), Betts-Miller-Janjic (P1C22), Grell-3 (P1C55) 2020 (top three panel) is represented in Fig. 5. In general, the WRF-ARW model with all three-cumulus parameterization schemes (CPS) was able to capture the distribution of 24-hour accumulated rainfall well as compared with the ERA5 re-analysis datasets for 4 days. It is important to see that the intensity of 24-hour accumulated rainfall captured by all CPS of WRF-ARW model is well and overestimated at some places over BoB during landfall and the oceanic region as compared to ERA5 reanalysis datasets. The 24-hour accumulated rainfall valid at 0000 UTC on 17-18 May 2020 from ERA5 reanalysis datasets and all CPS of WRF-ARW model shows heavy rainfall around the cyclone eye. However, the simulations for day 1 forecast from 0000 UTC on 17-18 May, day 2 forecast from 0000 UTC on 18 May 2020 capture the rainfall pattern, and position reasonably well by the Grell-3 scheme of WRF-ARW model (left top three panel).

The 24-hour accumulated rainfall by ERA5 reanalysis datasets valid at 0000 UTC on 19 May 2020 shows heavy rainfall (≥150 mm) around the Puri district of Odisha and moderate rainfall (25–150 mm) over Coastal districts of Gangetic West Bengal (East Medinipur, South and North 24 Parganas). Once again, all the CPS of WRF-ARW model has slightly over estimated the rainfall over the ocean with all three simulations. The simulations of 0000 UTC on 18-20 May of 72 hour forecast using all the CPS of WRF-ARW model captured the heavy rainfall around the Jajpur, Balasore, Cuttack, Mayurbhanj, Khordha and Puri districts. However, in comparison of all three CPS, Grell-3 scheme predicted the 24 hour accumulated rainfall during the above said period closer to the ERA5 reanalysis datasets.

The simulations of 18 May 2020 of 72 hour forecast (left middle) and 17 May 2020 of 96-hour forecast (left) agree reasonably well with ERA5 reanalysis 24 hour accumulated rainfall. Furthermore, simulations of 17-18 May 2020 can predict the distribution and intensity of rainfall very successfully. The WRF-ARW model with all three CPS simulated 24 hour accumulated rainfall specially Grell-3 scheme

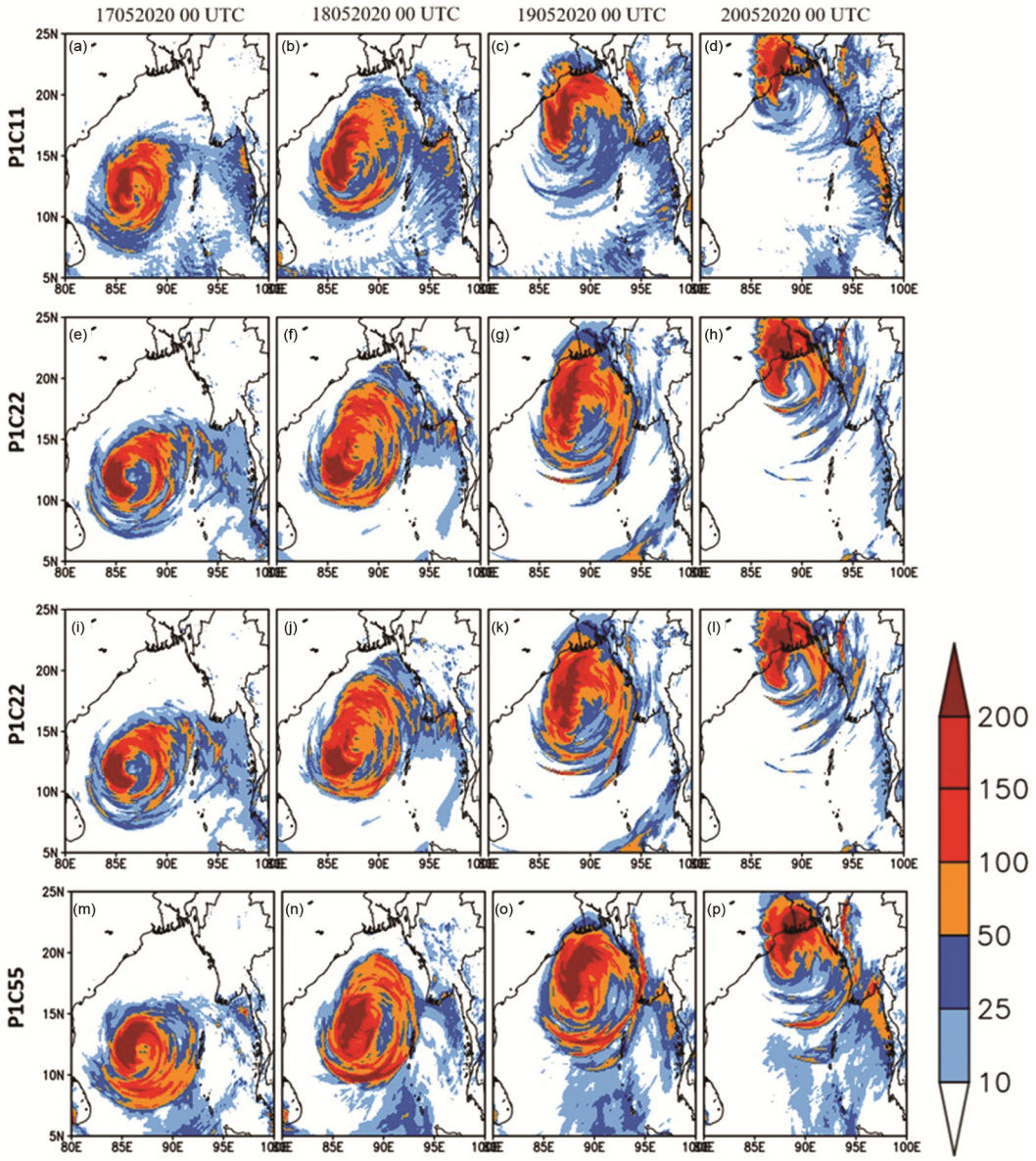

Fig. 5 — Rainfall (mm) from pre landfall (17 May 2020) to post landfall (20 May 2020) using three different cumulus parameterization schemes KF (P1C11), BMJ (P1C22), and Grell-3 (P1C55) of WRF-ARW experiment data and ERA5 reanalysis datasets

covers more area than ERA5 reanalysis datasets over West Bengal, Bangladesh. Thus, the comparison of ERA5 reanalysis and WRF-ARW model-predicted rainfall indicate that the Grell-3 cumulus parameterization scheme in WRF-ARW model is effectively capable to capture the rainfall in terms of position, distribution, and intensity.

From Figs. 4-5, It can be observed that the VIMT and rainfall around the tropical cyclone 'Amphan' over BoB during 16-21, May 2020 is very high. Further, by the above analysis using all cumulus parameterization schemes of WRF-ARW model and ERA5 reanalysis datasets, the relationship between rainfall and VIMT over BoB during this period has a high positive correlation, indicating a strong association between the two variables. Given the nature of tropical cyclones 'Amphan', which bring heavy rainfall and strong winds, the VIMT during the cyclone's passage over BoB is seen to be significantly higher than during normal weather conditions. The association of VIMT and rainfall patterns can provide valuable information about the dynamics of tropical cyclones and their interaction with local weather systems. This result analysis of impact of VIMT on rainfall can be further analysed to understand the specific impacts of tropical cyclones.

5 Conclusion

The experiments of WRF-ARW model including three different cumulus parameterization schemes Kain Fritsch (KF) Scheme, Betts-Miller-Janjic (BMJ) scheme, and Grell-3 scheme is an effort to examine the prediction accuracy of WRF-ARW model for SuCS 'Amphan' over the Bay of Bengal. WRF-Version 4.1.2 was used in this study to evaluate how well WRF cumulus parameterization schemes simulated the formation of the super cyclonic storm "Amphan" over the Bay of Bengal. The current investigation leads to the following findings.

The analysis of MSW and MSLP for SuCS 'Amphan' emphasize the significance of accurate convection schemes in enhancing prediction accuracy. On comparing all three cumulus parametrization schemes, the MSW root mean square error (RMSE) for Grell-3 and the KF convection scheme is around 11.51 m/s and 11.31 m/s, respectively. The Grell-3 scheme is better for prediction since it is closer to observed data during intensive stages, and the overall RMSE is also very near to the KF scheme, even if the KF scheme is exhibiting improved predictions in terms of MSW RMSE. The BMJ and Grell3 schemes are both less successful in predicting the MSLP of SuCS "Amphan" than the KF scheme, according to the RMSE error analysis. However, the Grell-3 scheme performs better MSLP during intense stages. The deviations from observed values of IMD highlight the critical role that the choice of convection scheme plays in the reliability of cyclone predictions, emphasizing the need for further research and advancements in modelling techniques to better understand and anticipate the behaviour of such formidable natural phenomena.

High value of Latitude versus height structure of PV is captured by all three-cumulus parametrization schemes. In Grell-3 scheme, high PV values extend to greater heights in the atmosphere when compared to both the KF and BMJ schemes, but goes upto less height as compared to ERA5 reanalysis datasets.

We also observed response between intensity of the SuCS ‘Amphan’ during pre-landfall and moisture transportation over the region of model through VIMT. All the three cumulus parameterization schemes captured high value of VIMT than ERA5 reanalysis datasets. It is found that Grell-3 scheme captured more moist flows and the 24-hours accumulated rainfall than KF and BMJ schemes after 17 May 2020, 1800 UTC. The relationship between VIMT and 24-hours accumulated rainfall is observed and concluded they are proportional to each other. Thus, Grell-3 scheme of WRF-ARW model predicted both VIMT and 24-hours accumulated rainfall well.

Therefore, it is concluded that Grell-3 cumulus parameterization scheme shows better prediction capabilities than KF scheme and BMJ scheme based on the above analysis of tropical cyclone ‘Amphan’. These experiments become a catalyst for continued research, aiming to enhance the model's accuracy and reliability in predicting the intensity of cyclones over the Bay of Bengal and similar regions. Critical factors affecting cyclone prediction encompass initial conditions, model resolution, and diverse parameterization schemes notably including realistic steering flow. Thus, enhancing the precision of predictions for tropical cyclone genesis, structure, and intensity is attainable by using more combination of different physical schemes in WRF-ARW model, refining initial conditions and employing advanced data assimilation techniques.

References

1 Anthes R A, Mon *Weather Rev*, 105 (1977) 287.
2 Bell M M & Montgomery M T, Mon *Weather Rev*, 136 (6) (2008) 2023.
3 Betts A K, *Quart J Roy Meteor Soc*, 112 (1986) 677.
4 Betts A K & Miller M J, *Quart J Roy Meteor Soc*, 112, (1986) 693.
5 Feliciano S, García-Valdecasas Ojeda M, Donaire-Montaño D, Rosa-Cánovas J J, Castro-Díez Y, Esteban-Parra M J & Gámiz-Fortis S R, *Atmos Res*, 299 (2024) 107175.
6 Grell G A & Devenyi D, *Geophy Res Lett*, 29 (14) (2002) 1693.
7 Grell G A & Freitas S R, *Atmos Chem Phys*, 14 (10) (2014) 5233.
8 Hausman S A, Ooyama K V & Schubert W H, *J Atmos Sci*, 63 (1) (2006) 87.
9 Atlas I, India Meteorol Dept, 11 (2) (2008) 1.
10 Janjic Z I, *Mon Weather Rev*, 122 (1994) 927.
11 Kain J S & Fritsch J M, *J Atmos Sci*, 47 (1990) 2784.
12 Kain J S & Fritsch J M, *Am Meteor Soc*, 24 (1993) 165.
13 Kalnay E, Kanamitsu M, Kistler R, Collins W, Deaven D, Gandin L, Iredell M, Saha S, White G, Woollen J, Zhu Y, Chelliah M, Ebisuzaki W, Higgins W, Janowiak J, Mo K C, Ropelewski C, Wang J, Leetmaa A, Reynolds R, Jenne R & Joseph D, *Bull Am Meteor Soc*, 77 (3) (1996) 437.
14 Kumar A, Kumar S, Kumar N, Lohan N & Bhatla R, *J Ind Geophys Union* 28 (2) (2024) 99.
15 Kumar A, Xalxo K L, Kumar S *et al, Pure Appl Geophys,* 181 (2024) 3375.
16 Michalakes J, Dudhia J, Gill D, Henderson T, Klemp J, Skamarock W & Wang W, *Atmos Sci*, 25, (2005) 156.
17 Mo K C & Higgins R W, *J Climate*, 9 (7) (1996) 1531.
18 Mohan M & Bhaskaran P K, *Atmos Res*, *139* (2014) 1.
19 Molinari J, Skubis S, Vollaro D, Alsheimer F & Willoughby H E, *J Atmos Sci*, 55 (16) (1998) 2632.

20 Murthy V S & Boos W R, *Quart J Roy Meteor Soc*, 145 (2019) 1968.
21 Ooyama K V, *J Atmos Sci*, 26 (1) (1969) 3.
22 Pattnaik S, Kar S C & Niyogi D, *Mausam*, *70* (4) (2019) 697.
23 Raju P V S, Potty J & Mohanty U C, *Meteor Atmos Phys,* 113 (2011) 125.
24 Rogers R, *J Atmos Sci*, 67 (1) (2010) 44.
25 Schubert W H & Alworth B T, *Quart J Roy Meteor Soc*, 113 (1987) 147.
26 Shapiro L J & Franklin J L, *Mon Weather Rev*, 123 (5) (1995) 1465.
27 Singh V, Srivastava A K, Gupta A, Konduru R T, Singh A, Singh S, Kumar A, Bisht D S & Singh A K, *Sci Total Env*, 951 (2024) 175501.
28 Skamarock W C, Klemp J B, Dudhia J, Gill D O, Barker D M, Wang W, Powers J G, *Natl Cent Atmos Res*, (2005) 1.
29 Skamarock W C, Klemp J B, Dudhia J, Gill D O, Barker D M, Duda M G, Huang X-Y, Wang W & Powers J G, *Natl Cent Atmos Res*, (2008) 1.
30 Stewart R H, *Texas A & M Univ*, (2003), 1.
31 Trenberth K E & Guillemot C J, *Climate Dynamics*, 14 (3) (1998) 213.
32 Trenberth K E, Fasullo J T & Mackaro J, *J Climate*, 24 (18) (2011) 4907.
33 Ullah K & Gao S T, *Adv Atmos Sci*, 29 (3) (2012) 501.
34 Verma S, Kumar S, Kant S *et al,* cyclones *Theor Appl Climatol,* 151 (2023) 311.
35 Wang H, Xu Z, Chen, X & Li J, *Atmos*, 13 (9) (2022) 1464.
36 Wang Y, *J Atmos Sci*, 65 (5) (2008) 1505.
37 Weisman M L, Skamarock W C & Klemp J B, *Mon Weather Rev,* 125 **(**1993) 527.
38 Yau M K, Liu Y, Zhang D L & Chen Y, *Mon Weather Rev*, 132 (6) (2004) 1410.
39 Zhang C, Wang Y & Xu H, *Geophys Res Lett*, 46 (3) (2019) 1485.